



AENSI Journals

Australian Journal of Basic and Applied Sciences

ISSN:1991-8178

Journal home page: www.ajbasweb.com



Coordinated Control of Power Converter in Wind Energy System Using Fuzzy Controller to Improve Power Quality

Mohanraj, M. and Rani Thottungal

Department of Electrical and Electronics Engineering, Kumaraguru College of Technology, Affiliated to Anna University Chennai, Coimbatore-641402.

ARTICLE INFO

Article history:

Received 19 August 2014

Received in revised form

19 September 2014

Accepted 29 September 2014

Available online 12 November 2014

Keywords:

Buck-Boost converter, Coordinated control scheme, Fuzzy logic, Efficiency, Hexagram Inverter, Wind Energy system.

ABSTRACT

This paper presents a coordinated control scheme (CCS) for hybrid resonant boost (HRB) converter and multilevel inverter. The proposed system is implemented for 1kW Wind Energy System (WES) power plant model. HRB control has been implemented using Fuzzy Logic Control (FLC). FLC algorithm reduces the output power oscillation and operates the wind system at maximum operating point. The HRB feeds a dc power to new 9-level inverter to ensure the quality of sinusoidal output. This nine level inverter reduces the harmonics in the system to the standard level. HRB and 9-level Inverter has been simulated using MATLAB. The simulation results are presented to validate the function of CCS.

© 2014 AENSI Publisher All rights reserved.

To Cite This Article: Mohanraj, M. and Rani Thottungal., Coordinated Control of Power Converter in Wind Energy System Using Fuzzy Controller to Improve Power Quality, *Aust. J. Basic & Appl. Sci.*, 8(18): 53-64, 2014

INTRODUCTION

The output characteristic of a WES depends on environmental conditions like wind velocity. The output characteristic has a unique maximum operating point at which the current-voltage product is greatest. Stand alone or Grid connected WES system should have a power controller to control the power flow to the load. The purpose of this is to ensure highest level of efficiency by operating WES at the maximum level, regardless of changes in external conditions. The simulink model of a WES with power tracking controller is investigated in Emad *et al.* (2011) to Sridhar *et al.* (2010). This controller typically consists of a step-up or step-down DC-DC converter. These converters are used to regulate the voltage and current at the load. It can be achieved by proper form of duty-cycle to the control circuit. Traditional converters and control algorithms are not highly effective in terms of ripple content, controller response to track the power from the WES in K.T. Chau *et al.* (2006) to Il-Oun Lee *et al.* (2012). To overcome this drawbacks, interleaved converter topology is introduced, which will improve the overall converter efficiency. The interleaved buck converter with reduced switching losses is explained in Yong Jung *et al.* (2011). Design and implementation of an interleaved boost converter for PV application is presented in Carl Ngai-Man Ho *et al.* (2012). Interleaved boost converter topology is implemented for fuel cell application in Ahmad Saudi Samosir *et al.* (2010). To reduce the overall switching losses of the converter, resonant converter topology like Zero Voltage Switching (ZVS) and Zero Current Switching (ZCS) have been introduced and presented in Bor-Ren Lin *et al.* (2011), Mahdi Rezvanyvardom *et al.* (2010) and Yao-Ching Hsieh *et al.* (2009). Combination of ZVS and ZCS is known as soft switching converter in Doo-Yong Jung *et al.* (2011) which improves the overall performance of the converter such as speed of response and conversion efficiency. The hybrid interleaved soft switching topology reduces the overall conversion efficiency as well as reduces the switching losses of the converter in Doo-Yong Jung *et al.* (2011).

Generally, dc-dc converter feeds dc power to inverters in a solar power plant and their control scheme is implemented using a dedicated digital controller Ahmad Saudi Samosir *et al.* (2010), Yao-Ching Hsieh *et al.* (2009) and Pongiannan *et al.* (2013). Then the power conversion in the inverter has also carried out using another digital controller in Prakash Singh *et al.* (2012), Muhammad Sadikin *et al.* (2012), Prajna Paramita Dash *et al.* (2012), Karuppanan and Kamala Kanta Mahapatra (2010), Pongiannan *et al.* (2011), Pongiannan *et al.* (2010) and Pongiannan *et al.* (2009). The multilevel inverter (MLI) topologies are investigated by the researchers due to its merits such as improved voltage levels and reduce rating of power switches.

Corresponding Author: Mohanraj, M., Assistant Professor, Department of Electrical and Electronics Engineering, Kumaraguru College of Technology, Affiliated to Anna University Chennai, Coimbatore-641402, Tamilnadu, India.

Design of Coordinated Control Strategy for HRB and MLI:

The block diagram of coordinated control strategy for HRB and MLI is shown in Fig.1. The proposed system considered for 1kW WES power generation. The peak power from the WES is about 960W, which may vary with change in climate condition. The specification of wind mill is presented in Table 1.

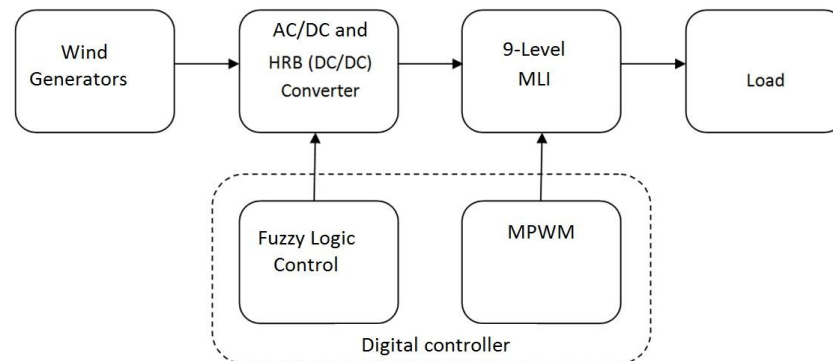


Fig. 1: Generalized block diagram of the proposed CCS.

The proposed HRB regulates the output of WES into the maximum level, by tracking the operating point using FLC algorithm. This FLC identifies the suitable duty cycle required by the converter to deliver the dc output with very low voltage ripple. The proposed converter also improves the overall conversion ratio and also reduces the switching losses of the converter. The regulated output from the HRB is fed to the 9 level Inverter. The control of this MLI is implemented using Modified pulse width modulation (PWM) scheme. The converter and MLI control is implemented using MATLAB software.

A. Design of Hybrid Resonant Boost Converter (HRB)

In general, the selection of Wind energy generator capacity is based on the load demand. In 1 kW WES systems the power generated will be less than the actual rating, in order to meet this demand by using HRB converter. The conversion efficiency of the traditional power converters are only 70% to 85% Dorin Petreus *et al.* (2010). Hence the traditional converters are failed to achieve the required output power with higher efficiency Dorin Petreus *et al.* (2010), Marcelo Gradella Villalva *et al.* (2009), Chee Wei Tan *et al.* (2008), Liu *et al.* (2004) and Hohm *et al.* (2003). But the proposed HRB converter has achieved the required power output by reducing the switching losses and effective switching operation of the converter switches as shown in Fig.2 explained in Doo-Yong Jung *et al.* (2011). The design of inductor and capacitors are made from the minimum and maximum output voltage variation from the WES (ie., $V_{in}(\min) = 34.6$ V and $V_{in}(\max) = 44.5$ V. Table-II shows the experimental data of a proposed system configuration. Nominal output voltage (V_{out}) and maximum output current (I_{out}) of the converter is to be fixed as 230 V and 5 A respectively.

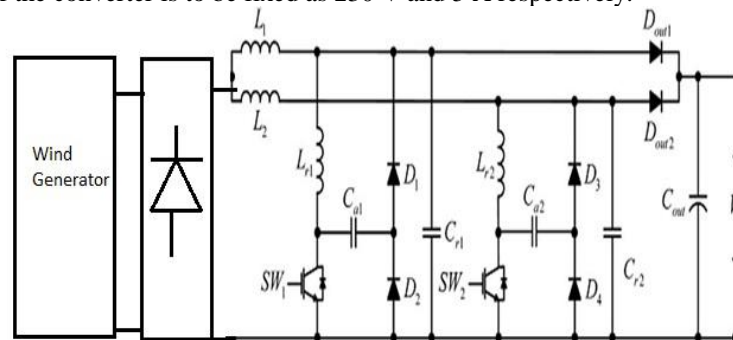


Fig. 2: Proposed Hybrid Resonant Boost (HRB) converter.

The nominal switching frequency of the converter switch is considered as $f_{sw} = 20$ kHz. The variation of duty cycle is calculated as follows.

$$D = 1 - \left(\frac{V_o(\text{panel})}{220} \right) \quad (1)$$

Hence the variation of the duty cycle to the HRB is from $D(\min) = 66.36\%$ to $D(\max) = 77.27\%$. Based on these parameters, inductor and capacitors of HRB are calculated.

Table 1: Parameters Of The 1kW Wind Energy System.

Turbine Type	Horizontal axis
Generator Type	Permanent Magnet
Number of Blades	3
Rotor Diameter	2.7m
Rotor Power coefficient	0.3
Rotor Swept Area	5.73m ²
Rated power	1000W
Rated Voltage	48V DC
Start-up wind speed	2.5m/s
Cut in wind Speed	3 m/s
Rated wind Speed	10.8 m/s
Braking wind speed	13 m/s
Max. safe wind speed	35 m/s
Rotor Speed	upto 420rpm

Table 2: Experimental Data From 1kW WES.

Windspeed (m/s)	Frequency of rotation (Hz)	Vac (v)	Current (A)	Vrms (V)	Vdc (V)
6	32	42.6	8	24.59512	57.55939
5	38.2	41.6	14	24.01777	56.20823
6.2	32	42.7	8	24.65286	57.69451
10.2	40.7	43.5	18	25.11474	58.77544
10	40.3	43.1	17	24.8838	58.23497
14	50	45	24	25.98076	60.80218
9	39	43.1	15	24.8838	58.23497
8.8	38.6	42.4	14	24.47965	57.28916
12	44.3	44.5	20	25.69209	60.1266
2.5	25.5	34.4	0	19.86085	46.47989
1	21	34.6	0	19.97632	46.75012
1.5	23.3	35.1	0	20.26499	47.4257
7	34	43.6	12	25.17247	58.91055

A. Design of HRB circuit Elements:**a. Inductor:**

Boost inductor can be selected in order to minimize the output current ripple by controlling sudden change in input current. It maintains the output as continuous and boosts the voltage and current when the converter switch is operated at higher switching frequency.

$$L_1 = L_2 = \frac{D \cdot V_{in} \cdot (1-D)}{(2 \cdot f_{sw} \cdot I_{out})} \quad (2)$$

The values of the resonant inductors are considered considering the input and output voltage across the converter switch as follows.

$$L_{r1} = L_{r2} = \frac{(V_{out} - V_{in} + V_d) \cdot (1-D)}{(f_{sw} \cdot \min(I_{out}))} \quad (3)$$

Peak value of inductor current can be determined in order to select the proper inductor value from equation (4).

$$I_{peak} = \frac{V_{in \max} \cdot D}{f_{sw} \cdot L} \quad (4)$$

Using (2)-(4), the values of inductors are calculated and the values are $L_1=L_2=89.69 \mu\text{H}$ and $L_{r1}=L_{r2}=56 \mu\text{H}$.

Where, D = Duty cycle to the converter

f_{sw} = Switching frequency of the converter in Hz

$V_{in(max)}$ = Maximum input voltage to the converter in Volts

V_{out} = Output voltage from the converter in Volts

V_d = Diode voltage drop in Volts

I_{out} = Output current from the converter in Amps

b. Diode:

The forward current rating required is equal to the maximum output current $I_f = I_{out}(\max)$ ie., 29.29A.

Schottky diodes have a much higher peak current rating than average rating. Therefore the higher peak current in the system is not a problem. The other parameter has to be checked in the power dissipation of the diode. It has to handle $P_d = I_f * V_f$ power rating. Where, I_f is average forward current of the boost converter diode and V_f is forward voltage of the boost converter diode.

c. Capacitor:

The minimum value for the input capacitor is necessary to stabilize the input voltage due to the peak current requirement of a switching power supply. The best practice is to use low equivalent series resistance (ESR) ceramic capacitors. Otherwise, the capacitor can lose much of its capacitance due to DC bias or temperature. The value can be increased if the input voltage is noisy. With external compensation, the equation (5) can be used to calculate the output capacitor values for a desired output voltage with low ripple voltage:

$$C_{out} > \frac{I_{out}}{V_{ripple} * f_{sw}} \quad (5)$$

Actual value of capacitance is selected higher than critical capacitance of the boost rectifier which is calculated using equation (5).

$$C_{r1} = C_{r2} = \frac{D_{min} * (I_{max} - I_{min})}{\pi^2 * L_r * f_{sw}} \quad (6)$$

In equation (6) considers the value of the resonant inductor which decides the current rating of the capacitor. The resonant capacitor value as shown in equation (6) is selected based on the maximum and minimum current in the converter legs. Using (2)-(4), the values of capacitors are calculated and the values are $C_{out}=100 \mu\text{F}$ and $C_{r1}=C_{r2}=10 \mu\text{F}$.

Fuzzy Logic Control:

Perturbation and observation (P&O) method is one of the most efficient methods among all the MPPT strategies. In general, P&O algorithm uses a fixed step size, which is determined by the accuracy and tracking speed requirements in Dorin Petreus *et al.* (2010). However, if the step size is increased for tracking speed-up, the accuracy is decreased. Also P&O fails to track the power under fast varying atmospheric conditions resulting in a comparatively low efficiency. These drawbacks of traditional P&O algorithm can be eliminated by varying the step size under varying atmospheric conditions. It will effectively reduce the power losses in the system and operate the PV system close to MPP. In this paper, Fuzzy based maximum power tracking method is proposed and is dedicated to find a simple, effective way to improve tracking accuracy and to overcome the drawbacks in traditional methods. Fuzzification includes the design of input and output membership functions. These functions are designed based on the prior knowledge. The two input and one output membership functions are illustrated in Fig.3, in which the firing angle of the converter is automatically varied according to operating point of a WES.

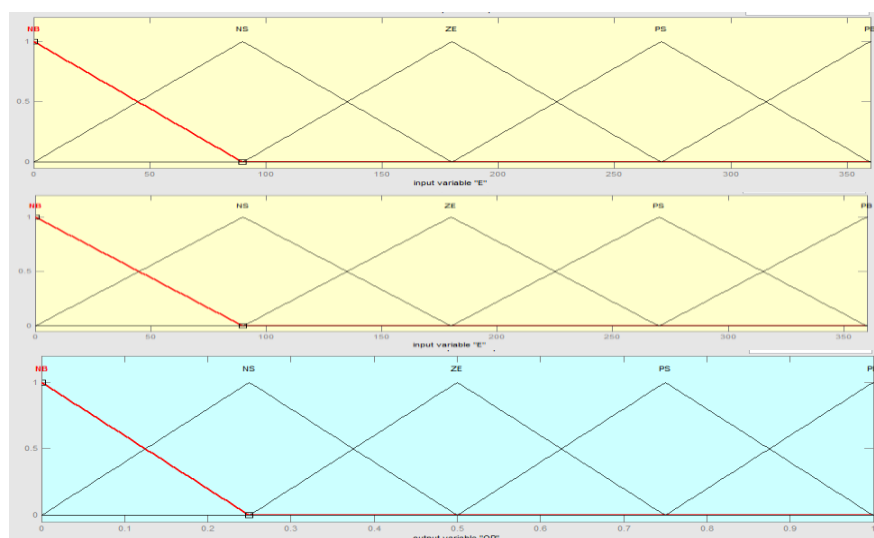


Fig. 3: Fuzzified input and output functions.

The maximum switching frequency of the HRB converter is fixed as 20 kHz. To reduce the output voltage ripples, the initial duty cycle to the converter is fixed as 66.36%. The voltage and current of the WES is sensed to find the MPP by calculating the power. Rules for the FLC implementation are presented in Fig.4. Hence the duty cycle of the converter has been changed according to fast varying climate conditions like wind velocity level and temperature.

CE/E	NB	NS	ZE	PS	PB
NB	NB	NB	NS	NS	ZE
NS	NB	NS	NS	ZE	PS
ZE	NS	NS	ZE	PS	PS
PS	NS	ZE	PS	PS	PB
PB	ZE	PS	PS	PB	PB

Fig. 4: Rules for the FLC algorithm.

The rule base defines the relationship between input and output membership functions. The control rules are evaluated by the inference mechanisms. Fig.4. Shows the rule base of fuzzy logic controller the linguistic variables used are NB-Negative Big NS – Negative small ZE- Zero PS- positive small PB -positive Big.

Modified Multi Level Inverter Topology:

This paper also presents a new nine level inverter topology for Wind Energy System application. To achieve 9-level, the traditional cascaded inverter topology needs 20 power switches and 24 switches in diode clamped arrangement. But, the proposed nine level inverter has only seven IGBT switches in the power circuit. Input V_{dc} from the HRB converter is divided into four levels using dc link capacitors of each $V_{dc}/4$ magnitude as shown in Fig.5. Four identical reference signals that are identical to each other with an offset that is equivalent to the amplitude of the triangular carrier signal were used to generate the PWM signals from the dc supply voltage. The operation of nine level inverter topology is explained and shown in Fig.6 (a)-6(i). and corresponding switching sequences are presented in Table 3. and Fig.7 presents Modified PWM switching patterns to the 9-Level inverter.

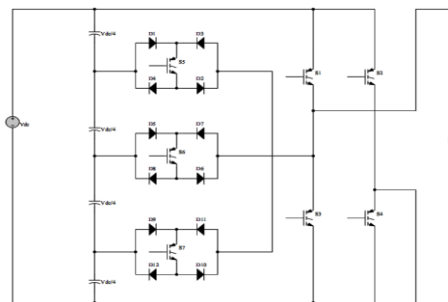
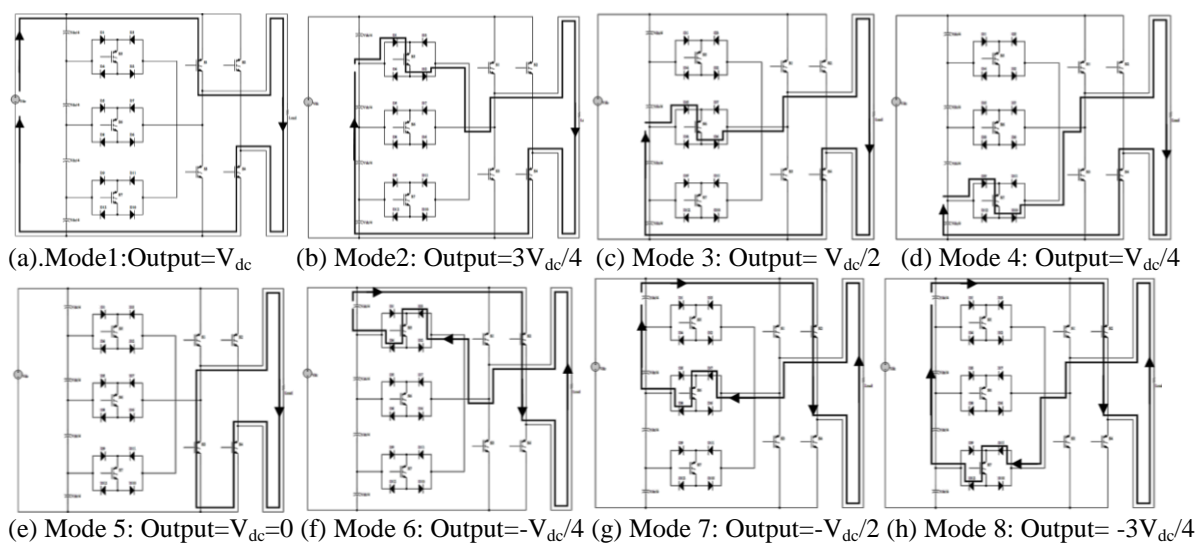


Fig. 5: Schematic of the 9-level inverter.



(a). Mode 1: Output = V_{dc} (b) Mode 2: Output = $3V_{dc}/4$ (c) Mode 3: Output = $V_{dc}/2$ (d) Mode 4: Output = $V_{dc}/4$
 (e) Mode 5: Output = $V_{dc} = 0$ (f) Mode 6: Output = $-V_{dc}/4$ (g) Mode 7: Output = $-V_{dc}/2$ (h) Mode 8: Output = $-3V_{dc}/4$

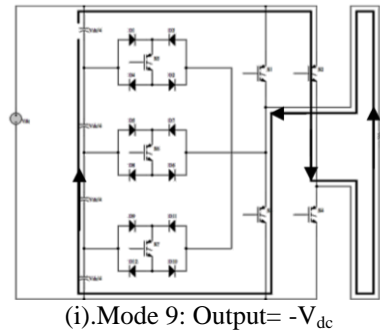


Fig. 6: Different operating modes of 9-level inverter.

The proposed 9-level inverter has four voltage divider capacitors such as C_1 , C_2 , C_3 & C_4 respectively as shown in Fig.5, which is powered by the HRB converter. These capacitor dividers provide the nine voltage levels by controlling the seven IGBT switches with flow control diodes, which are presented in Table 3.

Table 3: Switching Table for The Modified 9-Level Inverter.

Mode	Switching sequence	Voltage level
1	S_1 & S_4	$+V_{dc}$
2	D_1 , S_5 , D_2 & S_4	$+3V_{dc}/4$
3	D_5 , S_6 , D_6 & S_4	$+V_{dc}/2$
4	D_9 , S_7 , D_{10} & S_4	$+V_{dc}/4$
5	S_3 & S_4	$V_{dc}=0$
6	S_2 , D_3 , S_5 & D_4	$-V_{dc}/4$
7	S_2 , D_7 , S_6 & D_8	$-V_{dc}/2$
8	S_2 , D_{11} , S_7 & D_{12}	$-3V_{dc}/4$
9	S_2 & S_3	$-V_{dc}$

The 9-level has been achieved by operating the power switches at nine different modes. In the first mode, the nine level inverter operated at maximum positive voltage i.e., V_{dc} by operating the switches $S_1 \Rightarrow S_4$ as shown in Fig.6(a). voltage level has been reduced to the three-fourth at the second mode of operation by activating the switches in the following sequence $D_1 \Rightarrow S_5 \Rightarrow D_2 \Rightarrow S_4$ which is mentioned in Fig. 6(b). Similarly in the other modes the output voltage levels has been changed by selecting the capacitive voltage divider arrangement using the power switches as presented in Table 3.

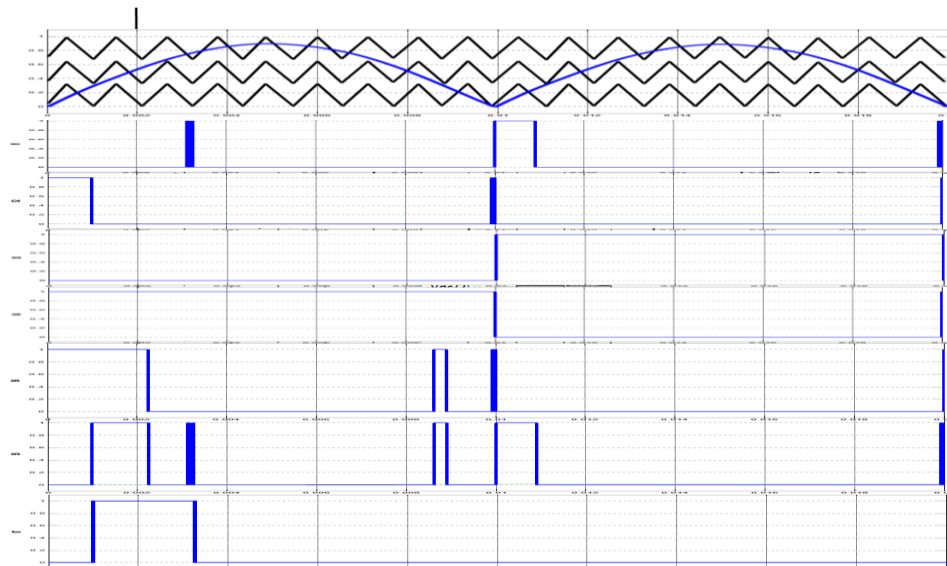


Fig. 7: Modified PWM switching patterns to the 9-Level inverter.

Implementation of this modified 9-level inverter topology has several advantages over the conventional MLI topologies. The proposed MLI have reduced number of power switches with low power rating. This may also reduces the switching losses in the inverter and reduces the THD at different operating frequencies (f_{sw}).

Implementation Of Coordinated Control Strategy:

In this coordinated control strategy, digital control of HRB and MLI are implemented in a single low cost digital controller. The implementation of boost converter topology is achieved using separate digital controller. Also the implementation of MLI topologies are done using separate controller. The main objective of the CCS is to minimize the number of controllers used in the hardware for effective control operation. The speed of the controller is also taken much care while implementing coordinated control logic. Because the control logic contains the FLC for HRB converter as well as the Modified PWM signals to the 9-Level inverter which runs parallel for the entire control operation.

Maximum power point tracking in Wind Energy System is a sensitive process, because the output of WES is affected by various factors like wind velocity, tip speed ratio etc. These effects may be few micro seconds, but the output of the WES system becomes very low or zero during this time. During low voltage tradition power conditioners are fails to maintain the operating point of WES and also generating output voltage oscillation in the DC to DC converter output. Hence the power to the Inverter or MLI is varied continuously. These factors have been considered while selecting the control algorithm and suitable controller for the real time implementation. The speed of the algorithm and its controller should be more. FLC algorithm has an ability to meet the above said requirement and control. It maintains the power within few micro seconds and also adjusts the duty cycle to the converter according to the power variation from the WES. Simultaneously the control of the 9-Level inverter topology has been done using Modified PWM technique. The operating speed of this controller is about $5\mu\text{s}$. Hence the variation of power from the WES is identified and controlled within short time.

Simulation Results:

The simulation study is carried out for HRB and 9-level inverter for different operating conditions. Finally the CCS for the HRB and 9-level inverter topology is simulated using MATLAB simulink environment. The output of the HRB converter with FLC is verified for the various input conditions like temperature and wind velocity. While compare with other resonant converter topologies like Zero voltage switching (ZVS) and Zero current switching (ZCS), the output of the HRB is improved to the maximum level.

A. Simulation of HRB:

The ZVS, ZCS and proposed HRB converters are modeled and simulated in MATLAB simulink environment. The WES parameters are given as input to the WES model in [5]. This model will provide the power according to the input variation like wind velocity. Based on the experimental data as shown in Table 2, design of converter elements, the duty cycle range are fixed and simulated. The simulink model of the HRB converter is shown in Fig.8 and the comparative result of the ZVS, ZCS and HRB are given in Fig.17. From the simulation study the efficiency of the HRB is increased to 97.7% and the output oscillations are damped out with the help of FLC algorithm.

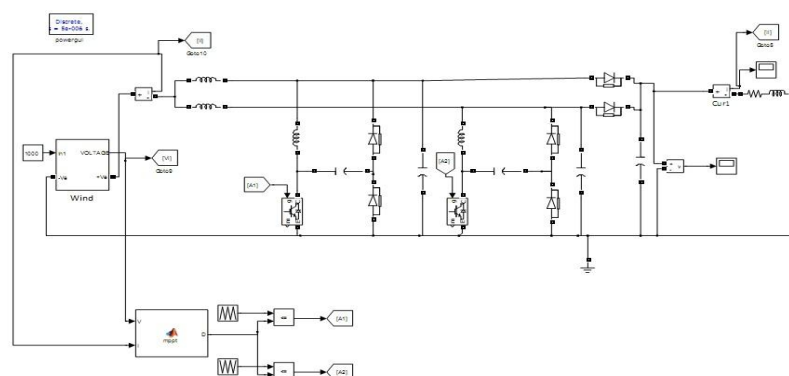


Fig. 8: MATLAB Simulink model of HRB converter.

Fig.17 shows the comparative results of the ZVS, ZCS and HRB converter output voltage waveforms at different wind velocities. From these results, it is observed that the ZVS converter output voltage of magnitudes 180 V, 195V and 208V settles at 0.25 sec with wind velocity of 3m/s, 6m/s and 12m/s respectively. ZVS have small voltage ripples at the output. Similar to this, ZCS converter took 0.1 sec to settle the output without any oscillations by having the voltage magnitude of 190V at 3m/s, 210 V at 6m/s and 220V at 12m/s.

Compared with these resonant converter topology, HRB have better conversion ratio and faster settling time which lead to higher efficiency and reduces switching losses. The output DC voltage from the HRB is maintained nearly 230 V, which settles within 20 ms at different input conditions.

B. Simulation of modified 9-level inverter topology:

The modified 9-level inverter topology using MATLAB simulink model is shown in Fig.9. The modified inverter topology was analyzed using different operating frequencies. The waveforms of the 9-level inverter with and without filter and THD are presented in Fig.10 to Fig.15. The digital PWM control of these switches increases the magnitude of the output voltage steps and also reduces the harmonic in the output.

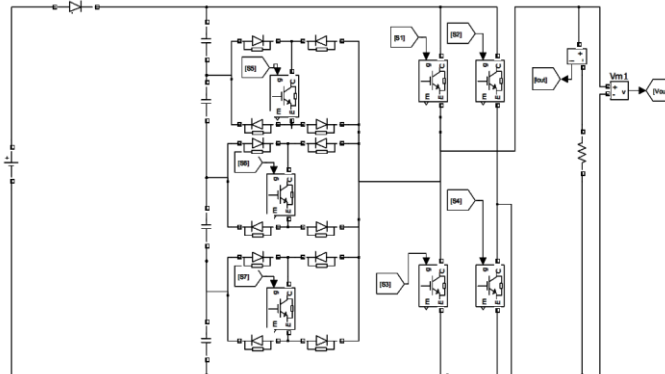


Fig. 9: MATLAB Simulink diagram of 9-Level inverter.

The MLIs is powered by the HRB converter. Since the operating frequency (f_{sw}) of the HRB is ranging from 10 kHz to 20 kHz, the 9-level inverter has been analyzed for the different operating frequency to maintain the coordination between converter and inverter output voltage levels. This will reduce the THD in the inverter output and also reduces the switching losses.

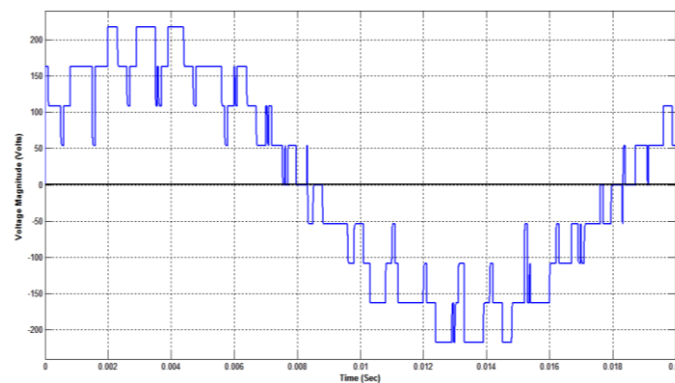


Fig. 10: Simulation Output of the 9-level inverter at $f_{sw} = 10$ kHz.

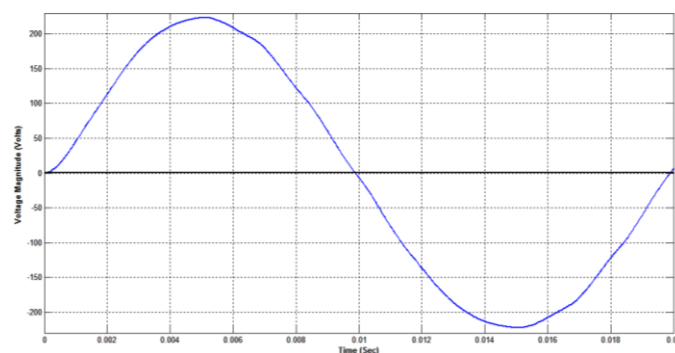


Fig. 11: Simulation Output of the 9-level inverter with filter at $f_{sw} = 10$ kHz.

The proposed 9-level inverter having the THD of 5.61% at $f_{sw} = 1$ kHz. The THD spectrum of the output voltage is shown in Fig.18 and the filtered output of MLI at 1 kHz frequency. When, $f_{sw} = 2$ kHz, the output voltage THD increased to 6.19% and the fundamental voltage magnitude is about 193.5 V. the voltage THD is reduces to 5.3% when f_{sw} increased from 2 kHz to 5 kHz. Since, the fundamental voltage magnitude reduced to 175.1 V. Hence the operating frequency of the inverter is considered as 10 kHz and 20 kHz, at these frequencies the voltage THD is reduced to standard level of 4.65% with the magnitude of 219.5V and is shown in Fig. 10 to Fig.15. .From these study the operating frequency (f_{sw}) of the inverter is also consider as 20 kHz to achieve the better coordinated control.

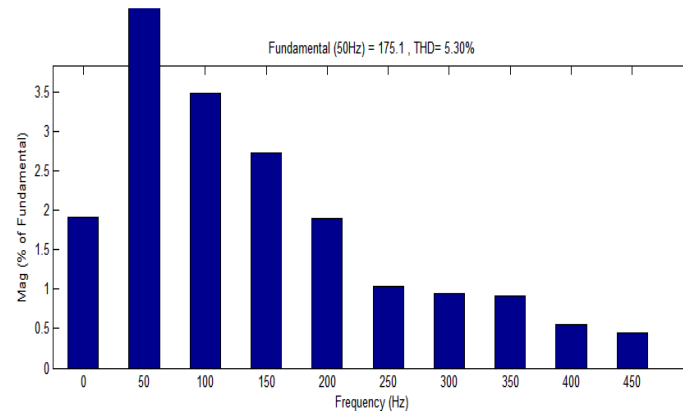


Fig. 12: THD spectrum of the 9-level inverter at $f_{sw} = 10$ kHz.

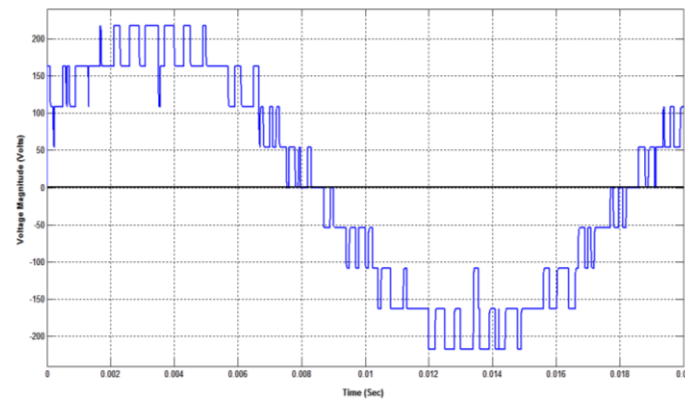


Fig. 13: Simulation Output of the 9-level inverter at $f_{sw} = 20$ kHz.

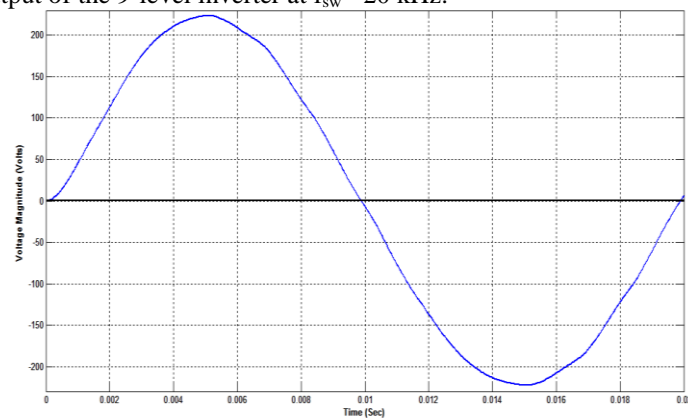


Fig. 14: Simulation Output of the 9-level inverter with filter at $f_{sw} = 20$ kHz.

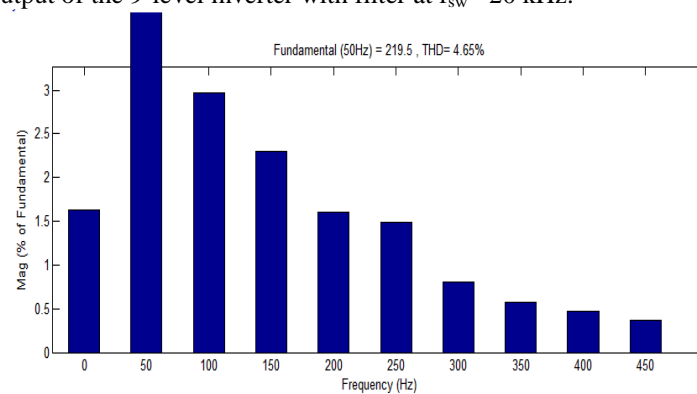


Fig. 15: THD spectrum of the 9-level inverter at $f_{sw} = 20$ kHz.

C. Simulation of CCS:

Coordinated control of modified 9-level inverter and proposed HRB is analyzed using MATLAB

simulation. The speed of the controller has been analyzed for the various parameter variations like wind velocity changes in the HRB and also the various operating frequencies to the 9-level inverter. The performance of the CCS is analyzed from the simulation results.

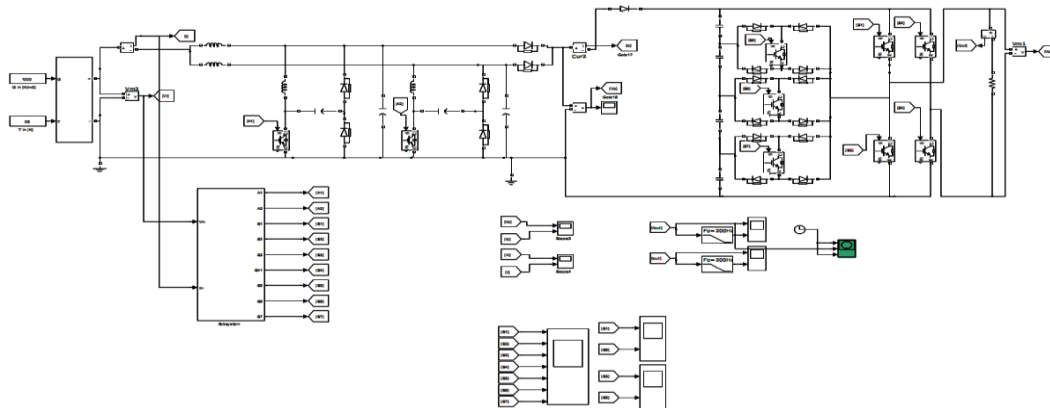


Fig. 16: MATLAB Simulink diagram of CCS.

Table 4: Switching Losses in the HRB & MLI.

Switching frequency (f_{sw}) (kHz)	Switching losses (Watts)	
	HRB	MLI
1	3.428	13.563
2	3.130	12.944
5	1.165	6.772
10	0.562	3.975
20	0.192	2.769

The switching losses in the HRB and MLI is analyzed for the various switching frequencies and input conditions, which is shown in Table 4. From the results, it is found that, the performance of the CCS is much better at 20 kHz frequency.

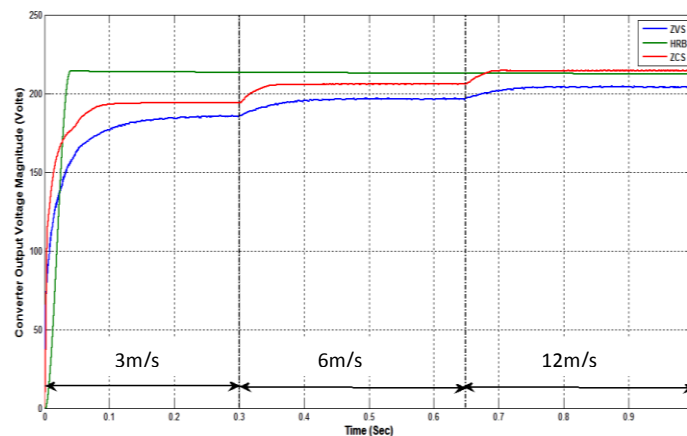


Fig. 17: Comparative waveform of the ZVS, ZCS and HRB under CCS at different wind velocities.

The performance of the resonant converters under fast varying wind speed in the CCS is shown in Fig.17. and the output of 9-level inverter is given in Fig. 12 to Fig.15.

The performance of the HRB converter remains same for the fast varying input conditions like wind velocity and temperature. Since, HRB took 20 ms to settle at the rated level as shown in Fig.17. The CCS is sensing the output of the HRB converter settles in a defined value, and then CCS controller generates the necessary pulse to the 9-level inverter switches.

Conclusion:

The CCS for the HRB and 9-level inverter has been designed and developed. The function of HRB, MLI and CCS are modeled using MATLAB Software. The simulation is carried for input conditions such as various wind velocities and switching frequencies. The FLC algorithm is implemented for MPPT control of HRB

converter and new PWM control to the MLI. The effectiveness of the control is verified through the simulation results. The CCS provides low THD, switching losses and improves overall efficiency of the converter into 97.9%. This modified nine level inverter topology also increases the output voltage level with reduced power rating of the switches. This CCS can be implemented in a low cost digital controller.

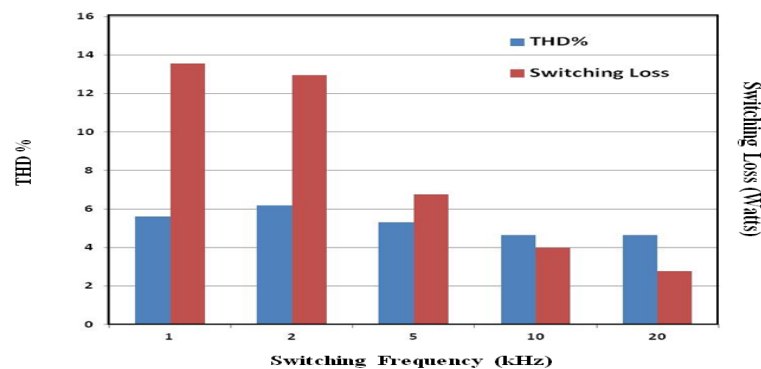


Fig. 18: THD and switching losses in the CCS at different switching frequencies.

REFERENCES

- Ahmad Saudi Samosir, Makbul Anwari and Abdul Halim Mohd Yatim, 2010. "Dynamic Evolution Control of Interleaved Boost DC-DC Converter for Fuel Cell Application", IPEC 2010.
- Bor-Ren Lin, Chia-Hung Chao and Chih-Cheng Chien, 2011. "Interleaved Boost-Flyback Converter with Boundary Conduction Mode for Power Factor Correction", Industrial Electronics and Applications (ICIEA), 2011 6th IEEE Conference on, 1828-1833.
- Carl Ngai-Man Ho, Hannes Breuninger, Sami Pettersson, Gerardo Escobar, Leonardo Augusto Serpa and Antonio Coccia, 2012. "Practical Design and Implementation Procedure of an Interleaved Boost Converter Using SiC Diodes for PV Applications", IEEE Transactions on power electronics, 27(6).
- Diego E. Soto-Sanchez and Tim C. Green, 2001. "Voltage Balance and Control in a Multi-Level Unified Power Flow Controller", IEEE Transactions on power delivery, 16(4).
- Doo-Yong Jung, Young-Hyok Ji, Sang-Hoon Park, Yong-Chae Jung and Chung-Yuen Won, 2011. "Interleaved Soft-Switching Boost Converter for Photovoltaic Power-Generation System", IEEE Transactions on power electronics, 26(4).
- Emad M. Ahmed and Masahito Shoyama, 2011. "Variable Step Size Maximum Power Point Tracker Using a Single Variable for Stand-alone Battery Storage PV Systems" Journal of Power Electronics, 11(2).
- Ersan Kabalci, Ilhami Colak, Ramazan Bayindir, Constantin Pavlitov, 2011. "Modelling a 7-Level Asymmetrical H-Bridge Multilevel Inverter with PS-SPWM Control", Acemp - Electromotion 2011, Istanbul – Turkey.
- Fang Zheng Peng, 2001. "A Generalized Multilevel Inverter Topology with Self Voltage Balancing", IEEE Transactions on industry applications, 37(2).
- Il-Oun Lee, Shin-Young Cho and Gun-Woo Moon, 2012. "Interleaved Buck Converter Having Low Switching Losses and Improved Step-Down Conversion Ratio", IEEE Transactions on power electronics, 27(8).
- In-Dong Kim, Eui-Cheol Nho, Heung-Geun Kim and Jong Sun Ko, 2004. Member, IEEE, "A Generalized Undeland Snubber for Flying Capacitor Multilevel Inverter and Converter", IEEE Transactions on industrial electronics, 51(6).
- Karuppanan, P. and Kamala Kanta Mahapatra, 2010. "FPGA based Cascaded Multilevel Pulse Width Modulation for Single Phase Inverter", Environment and Electrical Engineering (EEEIC), 2010 9th International Conference on, 273-276.
- Mahdi Rezvanyvardom, Ehsan Adib and Hosein Farzanehfard, 2010. "A New Interleaved ZCS PWM Boost Converter", IEE international conference on Power and Energy, Nov-29 to Dec-1, Kulalumpur, Malaysia.
- Mohan Reddy and T. Gowrیمانohar, 2012. "Comparison of Five Level and Seven Level Cascaded Multilevel Inverter Based DSTACOM for Compensation of Harmonics and Reactive Power using Instantaneous Real-power Theory", Emerging Trends in Electrical Engineering and Energy Management (ICETEEEM), 2012 International Conference on, 355-360.
- Muhammad Sadikin, Tomonobu Senjyu and Atsushi Yona, 2012. "DC-DC Type Bidirectional High-Frequency Link DC for Improved Power Quality of Cascaded Multilevel Inverter", IEEE conference on Power and Energy (PECon), 2-5 December 2012, kota Kinabalu Sabah, Malaysia.
- Pongiannan, R.K., M. Sathiyathan, A. Prakash, 2013. "FPGA Realization of Digital PWM Controller Using Q-Format Based Signal Processing," Journal of Vibration And Control, Accepted for publication.

Prajna Paramita Dash, Mehrdad Kazerani, 2012. "Harmonic Elimination in a Multilevel Current-Source Inverter-based grid-connected Photovoltaic System", IECON 2012 - 38th Annual Conference on IEEE Industrial Electronics Society, 1001-1006.

Prakash Singh, Sachin Tiwari, KK Gupta, 2012. "A New Transistor Clamped 5-Level H-Bridge Multilevel Inverter with voltage Boosting Capacity", Power India Conference, 2012 IEEE Fifth, 19-22, 1-5.

Sridhar, R., Jeevananathan, N. Thamizh Selvan and Saikat Banerjee, 2010. "Modeling of PV Array and Performance Enhancement by MPPT Algorithm" International Journal of Computer Applications, 7(5).

Yao-Ching Hsieh Te-Chin Hsueh and Hau-Chen Yen, 2009. "An Interleaved Boost Converter With Zero-Voltage Transition", IEEE Transactions on power electronics, 24(4).